Available online at www.sciencedirect.com

ScienceDirect

International Journal of Thermal Sciences 46 (2007) 164–171

International Journal of Thermal Sciences

www.elsevier.com/locate/ijts

Application of a heat pipe heat exchanger to dehumidification enhancement in a HVAC system for tropical climates—a baseline performance characteristics study

Yat H. Yau [1]

Department of Mechanical Engineering, University of Malaya, 50603 Kuala Lumpur, Malaysia

Received 4 October 2005; received in revised form 14 February 2006; accepted 14 February 2006

Available online 8 June 2006

Abstract

In Malaysia, humidity control is a common problem in built environments in tropical hot and humid climates as it is an important aspect of the maintenance of comfortable and healthy conditions within a controlled airspace. An 8-row thermosyphon-based heat pipe heat exchanger (HPHX) for tropical building HVAC systems was studied experimentally. This research was an investigation into how the sensible heat ratio (SHR) of the 8-row HPHX was influenced by each of three key parameters of the inlet air state, namely, dry-bulb temperature, relative humidity and air velocity. On the basis of this study, it is recommended that tropical HVAC systems should be installed with heat pipe heat exchangers for dehumidification enhancement.

Keywords: Heat pipe heat exchanger; Coolness recovery; HVAC systems; Dehumidification and sensible heat ratio

1. Introduction

Humidity control is a never-ending war in tropical hot and humid built environment, particularly, in Malaysia and Singapore. Yau and Tucker [1] mentioned that for many years, heat pipe heat exchangers (HPHXs) with two-phase closed thermosyphons, as shown in Fig. 1, have been widely applied as dehumidification enhancement and energy savings device in HVAC systems in Western countries. Hill and Jeter [2] modelled the effect of a HPHX on air-conditioning performance through a combination of a complete HPHX thermal node model and a model for the HVAC system implemented through performance maps. This research was conducted at Georgia Institute of Technology, Atlanta. Major increases in moisture-removal capability and efficiency through the application of this technology were seen improved in the range of 25–55%. In comparison, the redesign of a conventional evaporator produced a nominal decrease in sensible heat ratio in the range of 25–50% through the decrease of sensible capability but did not enhance latent capability or moisture-removal efficiency. This indicated that the application of a HPHX offered major improvements in humidity control and overall efficiency when compared to the usual practice of utilising a specially designed cooling coil in combination with reheat.

Despite many virtues practical operation of this device, the application of HPHXs in tropical countries is not wide spread, at least in Malaysia, Singapore, Indonesia and Brunei. Why is that so? One reason may be that almost all these experimental studies were done for cool and dry climate conditions.

A literature search has been carried out on theoretical and experimental research of HPHXs applied in HVAC (Heating, Ventilating and Air Conditioning) systems for the past 30 years (1970–2001), and it revealed that complete experimental research based on a Typical Meteorological Year (TMY) data for HPHXs applied in tropical climates for yearly operation of 8760 hours is virtually none. In addition, literature review further indicated that even research work related to energy recovery using HPHX carried out in sub-tropical climates are hardly found. Niu et al. [3] studied a HVAC system combin-

E-mail address: yhyau@um.edu.my.

[1] Yat H. Yau Ph.D., P.Eng. is a lecturer and M&E consulting engineer at the Department of Mechanical Engineering, University of Malaya, Kuala Lumpur, Malaysia.

1290-0729/$ – see front matter
doi:10.1016/j.ijthermalsci.2006.02.006

Nomenclature

AHU	air handling unit	
AC	air conditioner	
CWC	chilled water coil	
DBT	dry-bulb temperature	
WBT	wet-bulb temperature	
HPHX	heat pipe heat exchanger	
HVAC	heating, ventilating and air conditioning	
K	resistance coefficient	
$\dot{m}$	mass flow rate	$kg\,s^{-1}$
$\dot{Q}$	heat transfer rate	W
RH	relative humidity	

Subscripts

a	air
ac	air-conditioner cooling (process 2-3)
hpc	heat pipe pre-cooling (process 1-2)
hac	heat pipe and air-conditioner cooling (process 1-3)
hpr	heat pipe reheat (process 4-5)
NET	process 1-5
p1-3	process 1-3
p1-5	process 1-5

ing chilled-ceiling with desiccant cooling for maintaining the indoor air humidity within a comfort zone and to reduce the risk of water condensation on chilled panels. The results reveal that chilled-ceiling combined with desiccant cooling might conserve up to 44% of primary energy use compared to a conventional constant volume all-air system.

In a separate study, Zhang et al. [4] conducted a research on energy consumption for conditioning ventilation air and the annually performance of a membrane-based energy recovery ventilator (MERV) in Hong Kong. The results indicated that approximately 58% of the energy needed for cooling and heating fresh air might be saved yearly with an MERV, while only roughly 10% of the energy might be saved via a sensible-only energy recovery ventilator (SERV). In a similar study, Zhang et al. [5] conducted a study on a thermodynamic model built with an air moisture removal system incorporated a membrane-based total heat exchanger to estimate the energy use annually. The outcomes suggested that the independent air moisture removal could save 33% of primary energy.

Unfortunately, these research just mentioned above were conducted without a HPHX in the system even though these systems have some similarities in terms of heat transfer working mechanism compared to a system installed with a HPHX. Also, note that all these research work just described above were conducted in sub-tropical regions (Hong Kong and Southern China) with distinctive diagonal swing of outdoor air conditions (i.e. winter, spring, fall and summer seasons) annually compared to tropical regions with almost constant outdoor air conditions (i.e. hot and humid summer season only year-round).

Therefore, the relative dehumidification enhancement advantages of these new technologies for tropical HVAC systems are still in question. To this end, this investigation has been conducted and the major aim is to establish the baseline performance characteristics of the HPHX under conditions representative of those that would be experienced in a tropical climate for future research. The minor aim is to determine the dehumidification enhancement capability of a typical 8-row HPHX for yearly operation in tropical HVAC systems.

2. Overview of relevant theory

The HPHX evaporator section functions as a pre-cooler for the AC system and the condenser section as a reheating coil as shown in Fig. 2. By doing this the cooling capacity for the original system is re-distributed so that latent cooling capability of the conventional cooling coil is enhanced.

In hot and humid tropical climates, the moisture removal capability of the chilled water coil in the HVAC systems can be enhanced if the supply air is pre-cooled before reaching the chilled water coil. For instance, a typical HVAC system at aver-

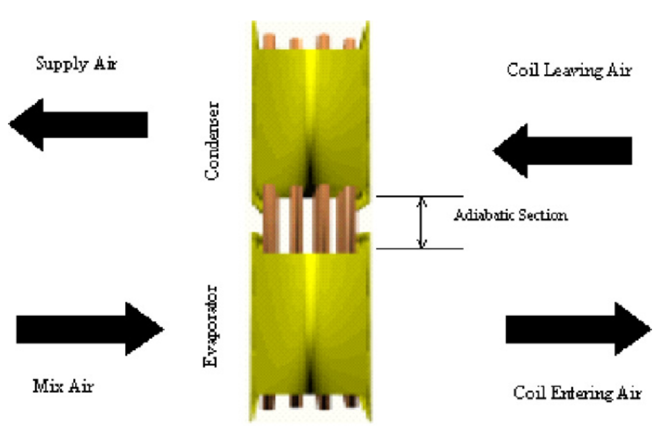

Fig. 1. A typical heat pipe heat exchanger (HPHX) applied in HVAC systems.

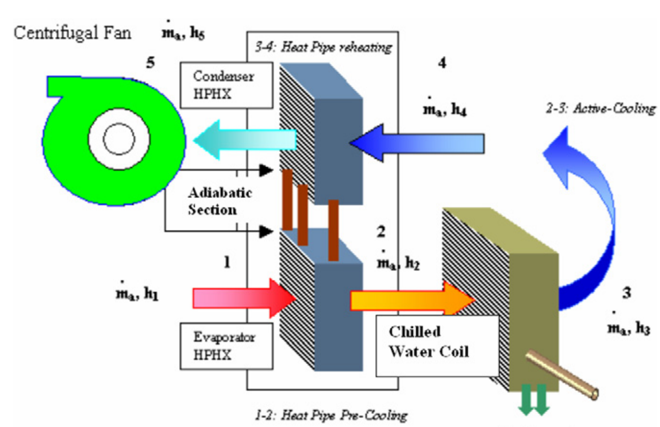

Fig. 2. Simple schematic diagram for HVAC model running with a HPHX [1].

age ambient condition of 32 °C and 58% relative humidity (RH) with total cooling load at 58.5 kW as shown in Fig. 3 can save 14.4 kW if HPHX is added into the HVAC system as shown in Fig. 4 [6]. Fig. 5 represents this situation with the present experimental air state numbering system superimposed.

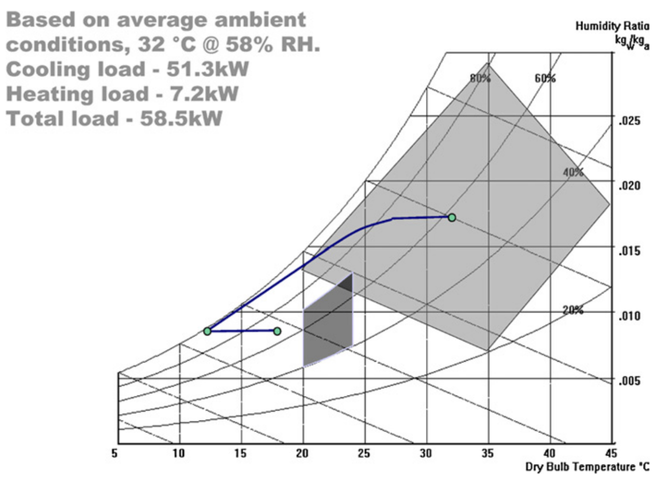

Fig. 3. Simple psychrometric processes for a typical HVAC system at average ambient conditions of 32 °C and 58% RH [6].

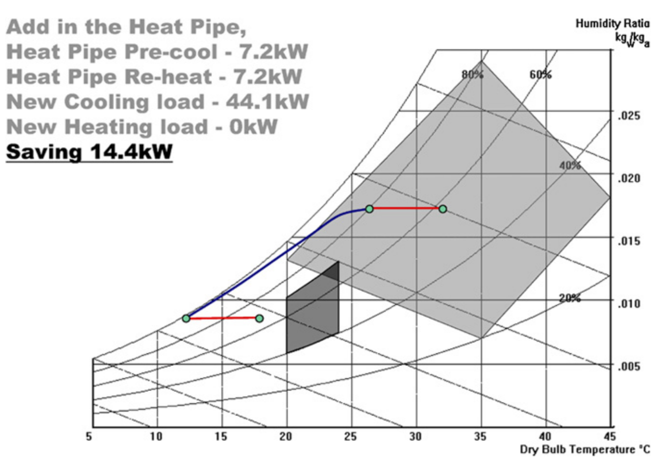

Fig. 4. Simple psychrometric processes for a typical HVAC system with an added HPHX at average ambient conditions of 32 °C and 58% RH [6].

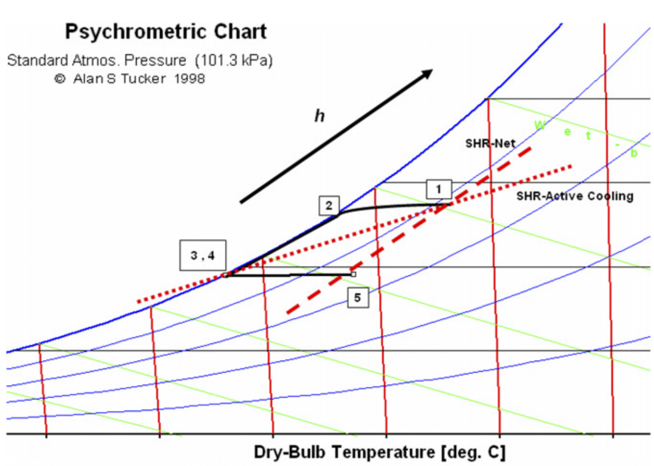

Fig. 5. HPHX overcooled and reheat processes in a HVAC system.

For illustrative purposes, the following have been assumed:

- The HPHX evaporator operates mostly sensibly and produces an exit state 2 which is close to saturation.
- The conventional cooling coil carries out its normal cooling and dehumidifying function (process 2-3), but with enhanced latent capacity because of the pre-cooling effect of the HPHX.
- Air transport between the cooling coil and the HPHX condenser occurs adiabatically (making states 3 and 4 coincident) and without leakage.
- The energy transfer rates in the two sections of the HPHX are equal and opposite {implying that $(h_1 - h_2) = (h_5 - h_4)$ since the air mass flow rates are equal}.
- The space has significant latent loads that would normally necessitate reheat in a conventional HVAC system.

Process 1-2 is the heat pipe pre-cooling and can be represented by:

$$\dot{Q}_{\text{hpc}} = \dot{m}_{\text{a}}(h_1 - h_2) \tag{1}$$

Process 2-3 is the air conditioner active cooling and can be represented by:

$$\dot{Q}_{\text{ac}} = \dot{m}_{\text{a}}(h_2 - h_3) \tag{2}$$

The total cooling load for the HVAC system is the combination of the HPHX pre-cooling and the AC active cooling, and can be represented by:

$$\dot{Q}_{\text{hac}} = \dot{m}_{\text{a}}\big[(h_1 - h_2) + (h_2 - h_3)\big] = \dot{m}_{\text{a}}(h_1 - h_3) \tag{3}$$

Process 4-5 is the heat pipe reheat load and can be represented by:

$$\dot{Q}_{\text{hpr}} = \dot{m}_{\text{a}}(h_5 - h_4) \tag{4}$$

It is clear that two advantages are provided by the HPHX—the free pre-cooling $(h_2 - h_1)$ and re-heating $(h_5 - h_4)$ processes. The pre-cooling process will enhance the cooling capability for the air conditioner and re-heating process will provide free reheat energy for the overcooled supply air.

In line with the way previous researchers have presented their data on HPHX performance [2,7], the sensible heat ratio was judged to be the most relevant in determining the capability of HPHX as a means of enhancing dehumidification. The sensible heat ratio, SHR, is defined as the ratio of sensible gains to total gains. In the research described in this paper, sensible heat ratios for the two-step cooling process (process 1-3) and overall net (process 1-5) are determined using the equations below.

For process 1-3, SHR is represented by:

$$\text{SHR}_{\text{Active Cooling}} = \dot{m}_{\text{a}} C_{\text{p1}-3}(T_1 - T_3)/\dot{m}_{\text{a}}(h_1 - h_3) \tag{5}$$

and Eq. (5) can be simplified to:

$$\text{SHR}_{\text{Active Cooling}} = C_{\text{p1}-3}(T_1 - T_3)/(h_1 - h_3) \tag{6}$$

where $C_{\text{p1-3}}$ is the moist air specific heat and can be represented to acceptable accuracy by:

$$C_{\text{p1-3}} = 1.005 + 1.84 W_{\text{Active Cooling}}\ \text{kJ}\,\text{kg}_{\text{a}}^{-1}\,\text{K}^{-1} \tag{7}$$

Since the dependence on humidity ratio, W is quite weak—W typically is of order $0.01\ \mathrm{kg_w\,kg_a^{-1}}$—a mean value for $W_{\text{Active Cooling}}$ can be used in Eq. (7), i.e.:

$$W_{\text{Active Cooling}} = (W_1 + W_3)/2 \tag{8}$$

Similarly, for process 1-5, SHR is represented by:

$$\mathrm{SHR}_{\mathrm{NET}} = \dot{m}_a C_{p1\text{-}5}(T_1 - T_5)/\dot{m}_a(h_1 - h_5) \tag{9}$$

and Eq. (9) can be simplified to:

$$\mathrm{SHR}_{\mathrm{NET}} = C_{p1\text{-}5}(T_1 - T_5)/(h_1 - h_5) \tag{10}$$

where, again, C_P may be evaluated from Eq. (7), this time using the appropriate mean humidity ratio:

$$W_{\mathrm{NET}} = (W_1 + W_5)/2 \tag{11}$$

3. Experimental set-up

A closed 'climate chamber' was used as the source of "outdoor" air for the experiments. The 'climate chamber' was 3.3 m long, 2.3 m wide, and 2.50 m high with a removable HVAC testing rig attached to it. This rig consisted of a removable 8-row HPHX, a removable CWC and a fixed variable speed fan with interconnecting duct work. The whole testing rig was insulated to minimise energy exchanges with the ambient environment. Polystyrene of 50 mm thickness and fibreglass (R value $\approx 1.5\ \mathrm{m^2\,K^{-1}\,W^{-1}}$) were applied as external insulation to the ductwork and components around the circuit.

Fig. 6 shows how the HPHX was installed in the testing rig for the present research. The HPHX was installed such that it pre-cooled the fresh air and reheated the overcooled air. The tropical hot and humid climates was provided by the under-floor air conditioning unit. The chilled water coil (CWC) was supplied with chilled water by the thermo-stated chilled water circulator with 2 kW of cooling capacity. The temperature of the chilled water in the circulator tank could be adjusted by a solid-state temperature controller, which provided an appropriate off-setting heat input to achieve the desired water temperature. The flow rate of the chilled water was able to be controlled by a screw type globe valve, with a resistance coefficient K of 8.2, in the circuit. The supply and return chilled water temperatures

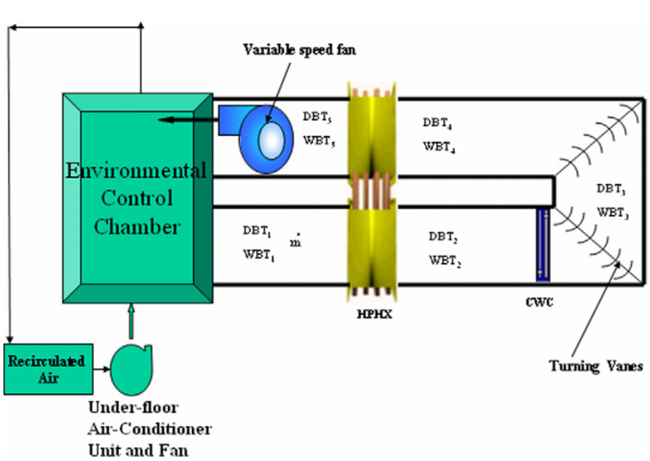

Fig. 6. Schematic diagram for the experimental set-up.

Table 1
Design specifications of the HPHX

Design	Specifications
HPHX Dimensions	405 mm wide, 945 mm high, and 375 mm deep
No. of coil rows	8 rows of 8 tubes, 5/8" (15.875 mm) OD × 0.48 mm copper
Centre-to-centre tube spacing	40.0 mm
Fins per inch	12
Fin blocks	4 (each with 2×8 tubes to allow easy access between rows for welding the headers to the coil block)

were monitored by two RTD probes. The air state maintained in the environmental chamber was drawn through HPHX evaporator. A LHG KANALFLAKT, model 315L, variable speed fan was installed to the left of the HPHX condenser, drawing air through the ducts, which all had a square section of 305 mm. The two air flows through the HPHX were such that it operated in a counter-flow configuration.

The detailed specifications for the HPHX are listed in Table 1. The HPHX was wickless, relying on gravitational return of condensate (i.e. a thermosyphon). The specification for the associated CWC had external dimensions 405 mm high, 470 mm wide, and 130 mm deep and an air face area of 305 mm × 305 mm. The CWC consisted of 2 rows of 8 tubes, having the same dimensions, spacing and finning as for the HPHX. The finned tubes connected to 1-1/4" (31.75 mm) copper headers and stubs.

The dry-bulb and wet-bulb and temperatures of the various air states were measured using type K thermocouples and the chilled water supply and return temperatures with RTD sensors. The output signals from these sensors were recorded and converted into degree Celsius via a Prema Data logging System [8]. During experimental runs the airflow rate was determined using a micro-manometer to measure the air static pressure drop across the circular orifice plate located at entry to the testing rig. This flow measurement system was pre-calibrated by carrying out a velocity traverse in the testing duct described in the next paragraph.

Tri-Sense Anemometer calibration was performed with both a micro-manometer (up to about 400 mm water gage) and a U-tube manometer to cover the full range of differential pressures generated by Annubar. The results show that an average the Tri-Sense Anemometer read approximately $0.08\ \mathrm{m\,s^{-1}}$ higher than the Annubar. The calibration procedure conformed to the requirements of ANSI/ASHRAE 41.2-1987 [9].

A total of 20 temperature sensors (18 type-K thermocouples and 2 RTD sensors) were calibrated in a thermostated water bath. The sensors were calibrated against a Prema Pt100 Immersion Probe 3012, having an accuracy of ± 0.005% [8], over the range of 10 °C to 50 °C. Cold junction compensation (CJC) was achieved automatically by means of a Prema Pt100 Probe 3011 [8] in an insulated box which also contained the terminal block into which the thermocouple wires were connected. The Tri-Sense relative humidity sensor calibration was achieved using saturated salt solutions for which the equilibrium relative humidity is well known for situations where the air flow is very low, or in closed chambers with no air flow. Additional details for instrument calibration procedures may be obtained from Yau [10].

4. Test conditions

For the HVAC system which was the focus of the broader scope of this research (a hospital operating theatre without recirculation located in Kuala Lumpur), it is the outdoor air state that would be experienced directly by the HPHX evaporator. Consequently, in order to obtain relevant performance data for a HPHX in this environment, it was necessary to cover a range of DBT and RH values appropriate to this Kuala Lumpur climate. The general climatic conditions of Kuala Lumpur, Malaysia, are mostly very hot with an average DBT at 20–33 °C and RH of 35–90%.

At the same time it was considered necessary to explore a range of coil face velocities representative of those which might typically occur in practice.

Thus, for this series of experiments, runs were performed as follows, with each of the three experimental variables altered one at a time:

- DBT values of 20 °C, 24 °C, 28 °C and 32 °C.
- RH values of 50%, 60%, 70% and 80%.
- Face velocity values in the approximate range of 1 to 2 $\mathrm{m\,s^{-1}}$ in 5 increments.

The RH value of $\leqslant$ 50% was not tested in this series of experiments because the experimental set-up (without dehumidifier) was not designed to achieve RH value of $\leqslant$ 50%, and also, because the proportion of hours per year for which Kuala Lumpur experienced RH values below 50% was very small. Thus, there was a total of 80 ($4 \times 4 \times 5$) experimental runs.

Because of some difficulties in achieving precise control of these parameters, there was some inevitable departure from run-to-run compared with the target values just listed. As will be seen, the resultant experimental data is recorded/plotted on an "as achieved" basis rather than an "as intended" basis. Nevertheless, for simplicity in presentation and discussion of the data, runs are grouped according to the above nominal values. Throughout each experiment, the system is allowed to achieve steady-state equilibrium conditions before data are collected. Additional details regarding the experimental set-up and operation may be found in Yau [10].

5. Results and discussion

The following sub-sections describe and discuss the HPHX performance results and the bias uncertainty in these results.

5.1. Performance results

A modified version of the psychrometric program [11] was developed to analyse data collected from these experiments. The data recorded by the Prema 3040 data logger were analysed automatically by the psychrometric software. The energy balance ratio (EBR), as indicated in Table 2, is defined as energy extracted from the hot air stream divided by energy transferred to the cold air stream. It is evident that EBR values, for all cases examined, are ranging from 0.89 to 1.11. These values implied that experimental uncertainty was present in these data because the EBR should be equal to unity if all energy extracted from the hot air stream was transferred to the cold air stream. Therefore, an error analysis was conducted in Section 5.2. The actual inlet air states for the HPHX evaporator are included in Figs. 7–10 for convenient reference.

The influence of inlet DBT for the HPHX evaporator on sensible heat ratio (SHR) for process 1-3 (SHR-Active Cooling) and process 1-5 (SHR-Net) are shown in Figs. 7 and 8, which are representative of results for the range of conditions tested.[2] The full set of data, covering all mass flow rates may be found in reference [10]. It is evident that, the SHR has been reduced by the HPHX as DBT at inlet to the HPHX evaporator increased. In other words, the results imply that moisture removal capability for the HVAC system with HPHX was increasing with inlet

Table 2
Energy balance ratio between the return and supply sides of the HPHX

Dry-bulb temperature [°C]	Energy Balance Ratio (EBR) = $\frac{\Delta h_{1-2}}{\Delta h_{4-5}}$			
	RH = 50%	RH = 60%	RH = 70%	RH = 80%
20	1.02	0.99	0.98	0.91
24	0.90	0.89	0.99	0.94
28	1.00	0.96	1.01	1.02
32	0.99	0.92	0.93	0.89
Mass flux rate at 1.6 $\mathrm{kg\,m^{-2}\,s^{-1}}$ (0.150 $\mathrm{kg\,s^{-1}}$)				
20	0.90	0.96	0.99	1.02
24	1.02	0.96	1.00	0.98
28	1.00	0.93	0.93	0.97
32	0.96	1.06	1.11	0.97
Mass flux rate at 1.9 $\mathrm{kg\,m^{-2}\,s^{-1}}$ (0.176 $\mathrm{kg\,s^{-1}}$)				
20	0.96	1.00	1.00	1.00
24	0.99	0.97	0.96	1.00
28	1.01	1.01	1.00	0.98
32	1.01	0.99	1.07	0.94
Mass flux rate at 2.1 $\mathrm{kg\,m^{-2}\,s^{-1}}$ (0.196 $\mathrm{kg\,s^{-1}}$)				
20	1.00	1.00	0.92	0.96
24	0.99	1.03	1.03	0.91
28	0.99	1.02	0.97	0.97
32	1.07	1.06	0.95	0.95
Mass flux rate at 2.2 $\mathrm{kg\,m^{-2}\,s^{-1}}$ (0.205 $\mathrm{kg\,s^{-1}}$)				
20	1.02	1.02	0.97	1.01
24	0.99	1.03	0.89	0.94
28	1.01	1.03	1.04	0.93
32	0.97	0.99	1.01	1.04

[2] The air mass flow rate (0.205 $\mathrm{kg\,s^{-1}}$) in Figs. 7–10 is actually the highest of the five, which were tested. This has been chosen here as being "representative" because of the fact that the corresponding coil face velocity is closest to that existing in the air handler of the operating theatre, which is the subject of detailed modelling in this research.

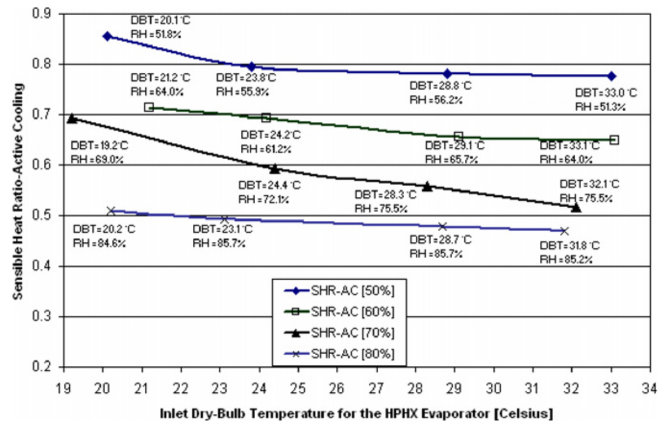

Fig. 7. The influence of inlet DBT for the HPHX evaporator on sensible heat ratio (SHR) for mass flux rate at 2.2 kg m^{-2} s^{-1}.

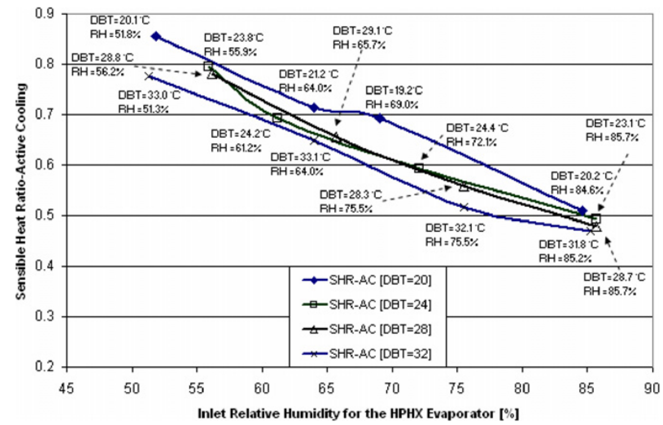

Fig. 9. The influence of inlet RH for the HPHX evaporator on sensible heat ratio (SHR) for mass flux rate at 2.2 kg m^{-2} s^{-1}.

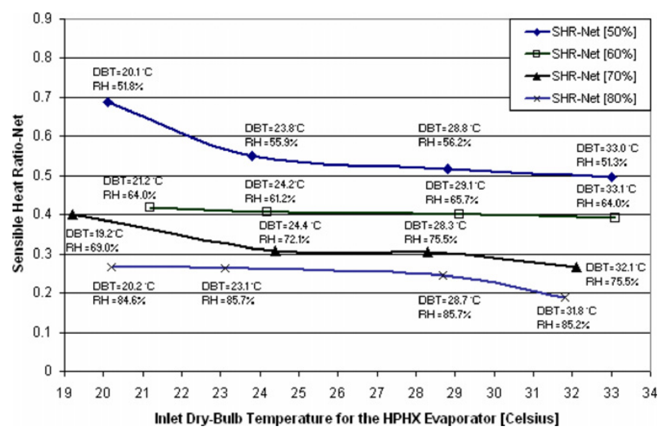

Fig. 8. The influence of inlet DBT for the HPHX evaporator on sensible heat ratio (SHR) for mass flux rate at 2.2 kg m^{-2} s^{-1}.

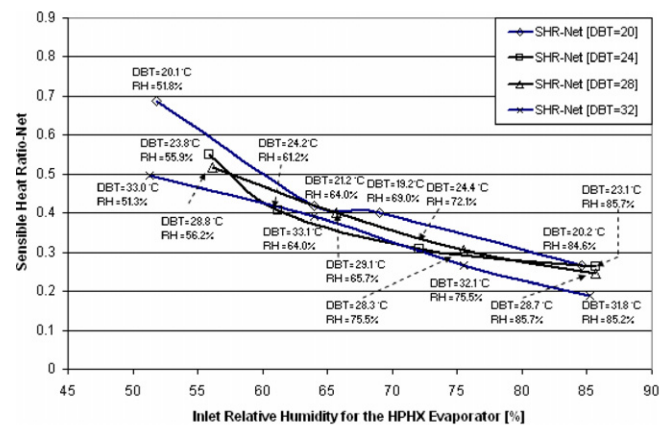

Fig. 10. The influence of inlet RH for the HPHX evaporator on sensible heat ratio (SHR) for mass flux rate at 2.2 kg m^{-2} s^{-1}.

DBT. Nonetheless, the influence of the inlet DBT on SHR is not so significant compared to the inlet RH.

Figs. 9 and 10 show the influence of inlet RH for the HPHX evaporator on sensible heat ratio (SHR) for process 1-3 (SHR-Active Cooling) and process 1-5 (SHR-Net). The full set of data may be obtained in reference [10]. Again, it was observed that for all cases examined, the SHR-Active Cooling and SHR-Net were reduced by the HPHX as inlet RH for HPHX evaporator increased. These results imply that the moisture removal capability for the HVAC system with HPHX was increasing with inlet RH for the HPHX evaporator increased. This was due to the fact that for the same inlet DBT for HPHX evaporator, the higher RH means smaller enthalpy change ($h_1 - h_2$) to achieve apparatus dew point (ADP) temperature, and therefore, the AC system, i.e. the HPHX evaporator and CWC, utilized a significant part of the cooling capacity for dehumidification (moisture removal) rather than sensible cooling (temperature reduction) as shown by process 2-3 in Fig. 5.

At the lowest combination of DBT and RH (i.e. 20 °C and 50%), however, for all mass flow rates, the SHR-Active Cooling was fairly high, ranging from 0.79 to 0.86. These results indicate that moisture removal capability of the cooling coils was not enhanced significantly by the HPHX for low DBT and low RH. This was attributed to the fact that under these conditions, the CWC utilised a significant part of its cooling capacity in sensible cooling. Nevertheless, the use of the HPHX in the system had reduced the SHR-Net to the range of 0.65 to 0.69 as compared to conventional cooling coils having a sensible heat ratio of 0.75 to 0.85 [12].

Figs. 11 and 12 show the influence of mass flux on sensible heat ratio (SHR) for process 1-3 (SHR-AC) and process 1-5 (SHR-Net), which are representative of results for the range of conditions tested.[3] The full set of data, covering all mass fluxes may be found in reference [10]. It was observed that for all cases examined, with the exception that for mass flux at ≈2.2 kg m^{-2} s^{-1} (i.e. the highest mass flux of the five which were tested), the increased mass flux had negligible influence on the SHR-AC and SHR-Net. The results are consistent with the observation, suggested that the law of mass conservation in the system by the forms of Eqs. (6) and (8), that SHR is not a function of mass flux rate. The apparent deviation at the highest mass flux (2.2 kg m^{-2} s^{-1}) may be attributed to the fact that at

[3] The DBT at 32 °C in Figs. 11 and 12 has been chosen here as being "representative" because of the fact that the DBT at 32 °C is closest to the ASHRAE 1% design method [10] for Kuala Lumpur climate.

Table 3
The bias uncertainties for the calibrated temperature sensors

Station	Max DBT [°C]	Max WBT [°C]	Min DBT [°C]	Min WBT [°C]	Bias uncertainty max [°C]	Bias uncertainty min [°C]	Error DBT [°C]	Error WBT [°C]
1	29.1	23.7	29.1	23.6	0.01	0.05	0.0	0.2
2	23.7	22.0	21.8	21.8	0.94	0.12	4.2	0.5
3	20.4	20.1	18.5	18.8	0.98[a]	0.62[a]	5.0	3.2
4	19.5	19.7	19.4	19.2	0.05	0.27	0.2	1.4
5	26.7	22.0	24.7	20.8	0.98	0.62	3.8	2.9

[a] It should be noted that bias uncertainties for station 3 (consisted of individual DBT and WBT sensors) were assumed to be the same as station 5 due to the fact that station 5 had the highest bias uncertainty values.

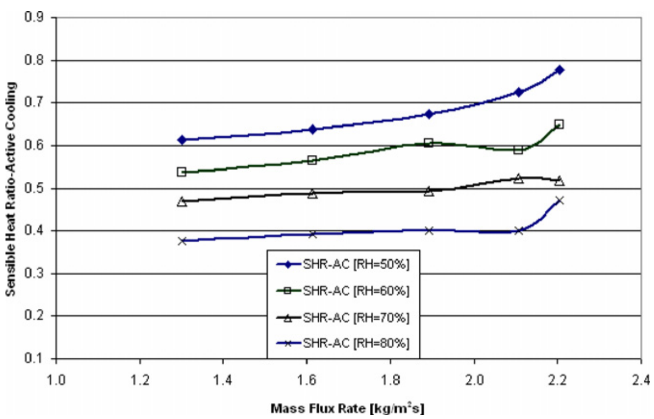

Fig. 11. The influence of mass flux rate on sensible heat ratio (SHR-Active Cooling) for DBT at 32 °C.

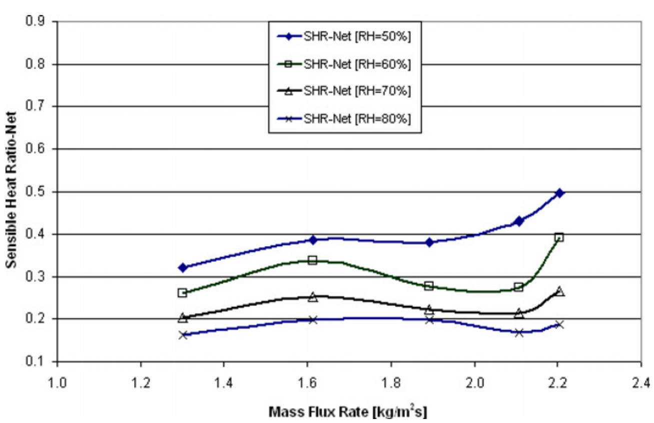

Fig. 12. The influence of mass flux rate on sensible heat ratio (SHR-Net) for DBT at 32 °C.

low air face velocity, moisture removal capability on the finned surfaces should be better than at higher air face velocity (because of the improved opportunity for contacting the cold fin surfaces) and, subsequently, the SHR generally is a little higher at high mass flux rate.

Although this study centred on tropical HVAC systems installed with heat pipe heat exchangers for dehumidification enhancement, it is good to mention that the size of refrigeration plants for HVAC systems installed with HPHXs could be expected to be reduced significantly because of the CWC moisture removal capability enhancement through re-distributing its latent part of the cooling capacity.

5.2. Error analysis

A bias uncertainty analysis was conducted for a representative experimental run for the inlet HPHX evaporator DBT at 29.1 °C, RH at 65.7% and mass flux rate at $\approx 2.2\ \mathrm{kg\,m^{-2}\,s^{-1}}$ ($0.205\ \mathrm{kg\,s^{-1}}$) and the results were given in Table 3. This representative experimental run was chosen because it was at the mid-range DBT and RH for the range of experimental runs. The mass flux rate at $2.2\ \mathrm{kg\,m^{-2}\,s^{-1}}$ was chosen due to the same reason as mentioned in Section 5.1.

The bias uncertainty for the SHR-active cooling and SHR-Net are 2.3 and 6.3% respectively. The bias uncertainty for the energy balance ratio (EBR) is significantly larger at 24%. These results suggested that non-uniform temperature distributions were present during this experimental run (Table 2). This could be traced to the fact that uneven cooling and heating were present for both chilled water coil and HPHX at stations 2, 3 and 5. The bias uncertainty for stations 1 and 4 were much lower than stations 2, 3 and 5 (see Table 3) because of better mixing in these two stations. The details of the bias uncertainty analysis can be found in reference [10].

6. Concluding summary

In this paper the baseline performance characteristics of the 8-row wickless HPHX used in a vertical configuration were established over a range of conditions appropriate for a tropical climate. The results would be used to build an empirical HPHX model in TRNSYS (Transient Systems Simulation Program) to simulate realistically the hour-by-hour psychrometric responses of an actual custom-built air handler unit (AHU) installed with or without added HPHXs in future research. The results of this work also could be used as an important guide for building services engineers and researchers who are intending to apply HPHXs as 'coolness' recovery and dehumidification devices in HVAC systems operating in tropical countries. The main conclusions from this work are:

(1) The experimental results demonstrated that for all cases examined, the overall SHR of the HVAC system was reduced from the maximum of 0.688 to the minimum of 0.188 by the HPHX as inlet DBT to the HPHX evaporator increased. These results implied that the moisture removal capability for the HVAC system with HPHX was increasing as inlet DBT for HPHX evaporator increased.

(2) For the nominal case of DBT $= 20\,^{\circ}\mathrm{C}$ and RH at 50% for all configurations of mass flow rates, the SHR-active cooling was fairly high, ranging from 0.786 to 0.856. These results indicated that the moisture removal capability was not enhanced significantly by the HPHX for low DBT and low RH.
(3) It was observed that for all cases examined, the SHR-active cooling and SHR-Net were reduced from the maximum of 0.856 to the minimum of 0.188 by the HPHX as inlet RH for the HPHX evaporator increased. These results implied that the moisture removal capability for the HVAC system with HPHX was increasing as inlet RH for the HPHX evaporator increased.
(4) On the basis of this study, it is recommended that tropical HVAC systems should be installed with heat pipe heat exchangers for dehumidification enhancement.

Acknowledgements

The author would like to acknowledge the full financial assistance from the Ministry of Foreign Affairs and Trade (MFAT), New Zealand, for research work to be conducted in New Zealand. Thanks are also extended to University of Malaya (MU) who awarded study leave and provided financial assistance to the author for research work to be conducted in the University of Canterbury. Also, the author wishes to thank Steelfort Engineering Ltd., Palmerston North, New Zealand, for donating an 8-row HPHX to be used in the present research. In addition, special thanks are extended to Mr. Ron Tinker, senior technical officer and Mr. Eric Cox, technical officer, at the Department of Mechanical Engineering, University of Canterbury, for their help during critical portions of the project.

References

[1] Y.H. Yau, A.S. Tucker, The performance study of a wet six-row heat pipe heat exchanger operating in tropical buildings, International Journal of Energy Research 27 (2003) 187–202.
[2] J.M. Hill, S.M. Jeter, The use of heat pipe heat exchangers for enhanced dehumidification, Proceedings of the ASHRAE Winter Meeting, January 23–26, 1994, New Orleans, LA, USA, ASHRAE Transactions 100 (1) (1994) 91–102.
[3] J.L. Niu, L.Z. Zhang, H.G. Zuo, Energy savings potential of chilled-ceiling combined with desiccant cooling in hot and humid climates, Energy and Buildings 34 (2002) 487–495.
[4] L.Z. Zhang, J.L. Niu, Energy requirements for conditioning fresh air and the long-term savings with a membrane-based energy recovery ventilator in Hong Kong, Energy 26 (2001) 119–135.
[5] L.Z. Zhang, D.S. Zhu, X.H. Deng, B. Hua, Thermodynamic modelling of a novel air dehumidification system, Energy and Buildings 37 (2005) 279–286.
[6] A. Westbury, Heat Pipes: The Benefits of Heat Pipes in Hot and Humid Climates, S&P Coil Products Limited, S.P.C. House, Evington Valley Road, Leicester LE5 5LU, England, http://www.spcoils.co.uk.
[7] J.M. Hill, Simulation of a variable speed air conditioner as a multiple loop thermal system, PhD thesis in Mechanical Engineering, Georgia Institute of Technology, September 1991, UMI, 300 N. Zeeb, Rd., Ann Arbor, MI 48106.
[8] Prema GmbH, Precision Thermometer PTM 3040 User Manual, Robert-Bosch-str. 6, D-55129 Mainz, Germany.
[9] ANSI/ASHRAE Standard 41.2-1987, Standard Methods for Laboratory Airflow Measurement, American Society of Heating, Refrigerating and Air Conditioning Engineers, Atlanta, 1987.
[10] Y.H. Yau, Energy savings in tropical HVAC systems using heat pipe heat exchangers, PhD in Mechanical Engineering Thesis, Department of Mechanical Engineering, University of Canterbury, October 2004.
[11] A.S. Tucker, On screen psychrometric chart, Department of Mechanical Engineering, University of Canterbury, Christchurch, New Zealand.
[12] D.B. Shirey III, Demonstration of efficient humidity control techniques at an art museum, in: Proceedings of the 1993 Winter Meeting of ASHRAE Transactions, January 23–27 1993, Chicago, IL, USA, ASHRAE Transactions 99 (1) (1993) 694–703.